Towards Improved IoT LoRa-WAN Connectivity using Broadband Omnidirectional Antennas

Mahmoud Wagih, *Member, IEEE*, and Peter Birley
School of Electronics and Computer Science, University of Southampton, U.K., mahm1m19@soton.ac.uk

***Abstract*—Despite the growing popularity of Long Range (LoRa) wide area networks (WANs), there is limited research on the antennas' influence on a node's connectivity. In this paper, the channel gain of an 868 MHz LoRa-Wan node in an urban environment is used to evaluate the performance of different antennas, as well as evaluate motion, elevation, and shadowing effects on the nodes connectivity. A dual-transmitter node with two tightly-coupled antennas is utilized to characterize the channel gain between the antenna-under-test, and multiple indoor and outdoor gateways over 1 km away, through the received signal strength indicator (RSSI). It is demonstrated that using a broadband UWB-inspired monopole implemented on an inexpensive cardboard substrate, the channel gain can be improved over commercially available whip antennas.**

***Index Terms*—Antennas, Internet of Things (IoT), IoT Nodes, LoRa-WAN, LP-WAN, Propagation, UWB antennas, wireless sensor networks.**

I. Introduction

With applications in industrial, environmental, and healthcare sensing, Sub-1 GHz Low Power (LP) Wide Area Networks (WANs) have attracted significant research interest as part of the exponentially growing Internet of Things (IoT). Agricultural monitoring, body area networks, and industrial automation are among the applications where LP WANs have been used to connect wireless sensor nodes (WSNs) [1].

Sub-1 GHz bands offer improved coverage in urban environments enabling LP WANs to have a kilometer-long range. Several compact antennas have been proposed for sub-1 GHz applications [2], [3], [4], [5], including dual-band printed circuit board (PCB) antennas for operation in the 433 and 868 MHz frequency bands [3]. Moreover, a range of antenna designs based on logos [3], as well as wearable textile-based [4], [5] have been developed for sub-1 GHz IoT applications. Most of these antennas have been experimentally characterized quantifying their gain and radiation efficiency. A reconfigurable-radiation patterns antenna was also proposed for sub-1 GHz applications, for tunable line of sight (LoS) and non-LoS improvements [2]. However, the impact of such gain, bandwidth, and efficiency figures on the connectivity in an IoT WAN were not experimentally investigated.

Propagation in IoT sub-1 GHz LP WANs has been studied in a variety of scenarios using off-the-shelf WSN hardware. For instance, the cumulative distribution formula (CDF) of the signal to noise ratio (SNR) was used to evaluate the dual-band antenna proposed in [3] against a commercial 868 MHz antenna. The off-body radiation patterns of a textile substrate integrated waveguide (SIW) antenna were validated in a real-world environment for body-to-body LoRa links up to 500 m with the wearable and gateway antennas aligned, correlating the received signal strength indicator (RSSI) to the radiation patterns measured in an anechoic chamber [6]. A body-to-gateway measurement campaign was later carried out demonstrating the advantages of single-in multi-out (SIMO) diversity in improving the wearable body-gateway link [7]. Nevertheless, in the aforementioned measurement campaigns, a single antenna was used and the impact of different WSN antenna's gain and bandwidth was not investigated.

In this paper, the performance of an IoT LoRaWAN node is evaluated through the RSS in a multitude of scenarios including movement, human shadowing, elevation, and indoor-outdoor links. In the aforementioned cases, a commercial whip antenna and a broadband monopole implemented on a low-cost cardboard substrate are compared showing that the broadband omnidirectional monopole can improve the nodes' connectivity. In Section II, we present the antennas' bandwidth and radiation pattern characterization, with the detailed LoRaWAN propagation measurements in a real-world IoT network in Section III.

II. Antennas Properties and Measurements Setups

A. Antenna Parameters Simulation and Measurements

Two antennas are considered in this work, the first is a components off the shelf (COTS) inductor-loaded whip-style monopole (Taoglas antenna with 16.8 cm length) designed to cover the 868 MHz ISM-band with a VSWR$<$1.5. The second antenna is an Ultra-wideband (UWB)-inspired disc monopole [8]. The disc monopole has been scaled to cover the sub-1 GHz 868/915 MHz bands [9], and is implemented on an inexpensive cardboard substrate using conformable copper films. The disc is fed using a 50 Ω microstrip line with a coaxial interface to connect to the test nodes. Despite the frugal construction of the antenna, it is not expected to influence the antenna's S_{11} and radiation patterns, as demonstrated experimentally. The substrate's dielectric properties were characterized using a T-resonator around 1 GHz as ϵ_r=1.2 and tanδ=0.032. Fig. 1 shows the a photograph and dimensions of the two-element cardboard antenna. Two antenna elements are implemented to connect to two separate LoRaWAN transceivers, which enables factoring in device variations for co-located nodes.

This work was supported by the UK EPSRC under grant EP/P010164/1.

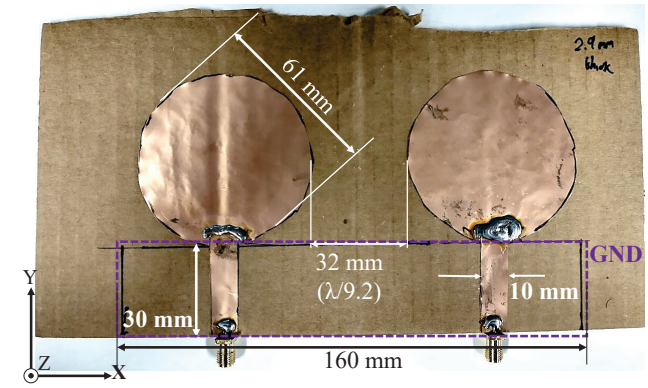

Fig. 1. Photograph and dimensions of the two-element cardboard monopole.

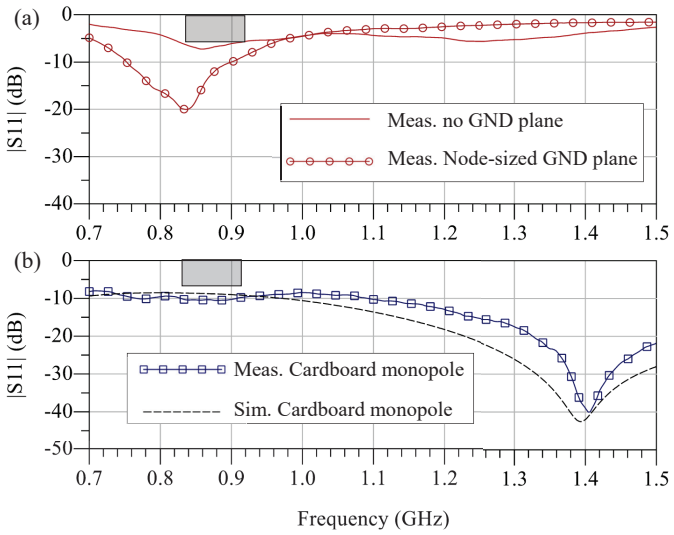

Fig. 2. Reflection coefficient of (a) COTS 868 MHz monopole; (b) UWB-inspired monopole.

Both antennas have been experimentally characterized using a Rhode & Schwarz ZVB4 Vector Network Analyzer (VNA). Fig. 2 shows the measured reflection coefficient of the COTS and UWB-inspired monopole, as well as the CST Microwave Studio-simulated response of the disc monopole. While the simulated antenna's S_{11} is higher than -10 dB, LoRaWAN transmitters operating in high-power mode (with a 20 dBm output) can withstand a VSWR of 3:1. As a result, an $S_11 < -6$ dB is sufficient for "matched" operation, unlike conventional high-gain amplifiers which require an $S_{11} < -10$ dB. From Fig. 2(a), it can be observed that as the COTS monopole does not contain a ground plane, its S_{11} is highly dependent on the size of the ground plane of the node. The node-sized ground is 7.5×6.5 cm, which matches the size of the double-sided ground plane on the LoRaWAN PCB. As the two monopole elements are closely spaced, the mutual-coupling S_{21} between both elements was measured experimentally and was found to be under -10 dB.

The radiation patterns of the UWB-inspired monopole were simulated in CST as well as measured in an indoor echoic

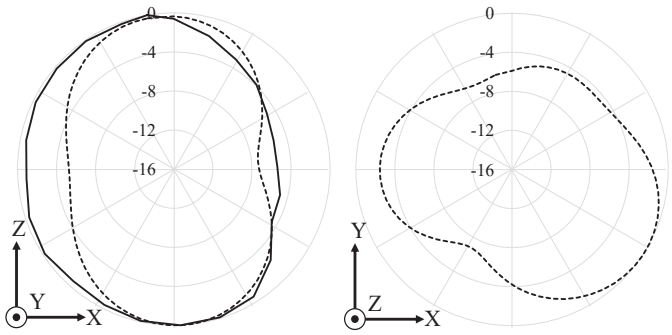

Fig. 3. Simulated (dashed) and measured (solid) radiation patterns of the disc antenna at 868 MHz over the elevation XZ and azimuth (YZ) plane.

environment with VNA time-domain gating [10]. Fig. 3 shows the simulated and measured patterns over the elevation XZ plane, and the simulated pattern over the azimuth YZ plane, verifying the omnidirectional coverage with a minimum gain over -10 dBi in all directions. The antenna's cross-polarized patterns were not measured due to unavailability of experimental facilities. The antenna's omnidirectional patterns are expected to improve the nodes' connectivity compared to a conventional $\lambda/2$ dipole or $\lambda/4$ monopole antenna, which exhibit a radiation null along their vertical axis [11].

B. LoRaWAN RSS Measurements Setup

The AUTs have been connected to a LoRaWAN node based on the COTS RFM95W LoRaWAN module. The test node is comprised two LoRaWAN transceivers and Arm Cortex-M ST32 microcontroller units. By including two transceivers, the effects of device variations on the RSS and number of successfully transmitted packets can be investigated. The nodes have been programmed to transmit at 14 dBm. Unlike previous works were a single custom gateway was used at a high duty-cycle [6], the nodes were connected to The Things Network (TTN) using LoRaWAN. By connecting the nodes under test to TTN, the received packets adhere to spectrum regulations as well as duty-cycle limits such as the 30 seconds daily limit on air time.

The experiments were carried out in Southampton, U.K. (coordinates: 50.939472, -1.397901), as shown in Fig. 4. Test location (a) enables the nodes, located outdoors under a trees cover, to connect to a nearby indoor gateway approximately 15 m away (Gw1), as well as the further away network of outdoor gateways located on buildings' roofs (GW2-7). In location (b), the node is positioned indoors close to a window, in relatively close proximity to the outdoor gateways Gw3-7. Unlike previous surveys, the two test locations enable the TTN RSS values to capture a variety of external factors such as elevation, building shadowing, and distance between the node and the gateways. For instance, while the body-to-body propagation of a mobile Lora node based on an SIW antenna was investigated over approximately 2.2 km distance [6], the experiments reported in this section investigate two additional factors. Firstly, multiple gateways are present in

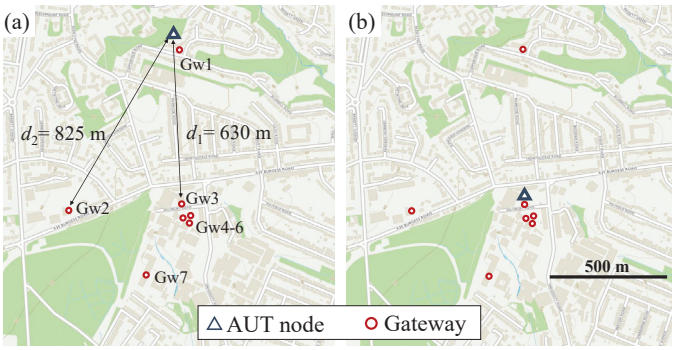

Fig. 4. The two test positions (a) and (b) of the antenna-under-test (AUT) node relative to the surrounding gateways, center coordinates: 50.939472, -1.397901.

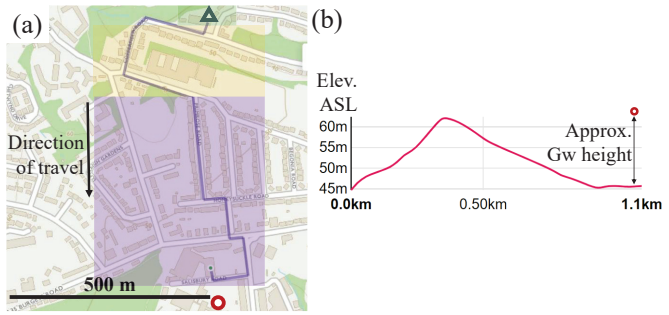

Fig. 5. The mobile nodes test location: (a) the 1.2 km walking route, shaded regions correspond to the RSS in Fig. 9; (b) elevation plot in the direction of travel.

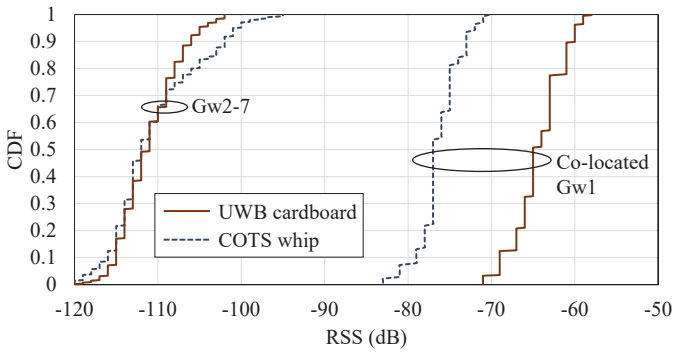

Fig. 6. Measured RSS of the nodes in position (a) from Fig. 4 for the co-located Gw1 and the further away Gw2-7.

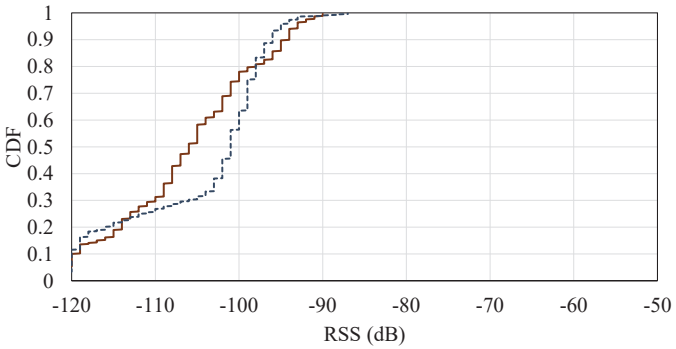

Fig. 7. Measured RSS of the nodes in position (b) from Fig. 4 for packets received by Gw2-7.

the surroundings of the node. Secondly, there is no LoS link between the node antennas and the gateways. Finally, unlike the experiments reported along a water canal free of building as well as hills [6], the measurement locations involve diffraction around multiple hills as well as buildings. A previous survey was conducted around the same location in 2017 [12], but only dealt with a single gateway and static RSS values as opposed to observing time variations, which were found in other works to be highly periodic and cannot be fully attributed to specific environmental conditions [13].

To further investigate the effects of elevation, movement, and shadowing, the path shown in Fig. 5(a) is traversed on foot to observe the RSS variations. As observed in Fig. 5(b), the existence of a hill between the nodes and Gw3-6 will introduce significant variations to the distance-RSS relation. The results of the measurements campaign in these three scenarios are detailed in the next section.

III. Network-Level Antenna Characterization

The CDF of the nodes' RSS is used to evaluate the wireless link in its two stationary positions shown in Fig. 4 (a) and (b). In Fig. 6, the CDF of the RSS for both the COTS whip antenna and the UWB-inspired monopole are shown for position (a). The CDF for the RSS in position (b) is shown in Fig. 7.

For the co-located indoor gateway (Gw1), it can be observed in Fig. 6 in the CDF of the measured RSS that the broadband monopole exhibits a significantly higher RSS with a mean RSS that is over 10 dB higher than its COTS counterpart. On the other hand, as the distance increases, both nodes exhibit comparable mean RSS values when transmitting to the further away outdoor gateways (Gw2-7). When both nodes are located indoors, i.e. setup (b), their RSS is comparable with a higher standard deviation for the COTS whip antenna. Moreover, the mean RSS at Gw2-7 improves by about 7 dB, relative to position (a), despite the distance between the nodes and Gw2-7 dropping by over 90%.

Comparing the RSS CDF in Fig. 6 and 7, it can be observed that when the node is in position (b), i.e. very closely located to Gw3-6, the mean RSS is around 7 dB higher than when in position (a). To explain, the node and Gw3-6 are separated by 680 m in position (a), and around 20 m in position (b), this corresponds to around 30 dB lower path loss when using the LoS free-space loss formula, which does not include the buildings shadowing or the hill, observed in Fig 5(b), which obstructs the path between position (a) and Gw4-6. Nevertheless, when the node is moved closer to Gw4-6, its mean RSS improves by less than 10 dB, which highlights that buildings shadowing in a dense non-LoS link can be more significant the distance between the node and gateway. Furthermore, over 10% of the packets having an RSS under -120 dBm and, a significantly higher standard deviation is observed. This is attributed to the higher density of buildings and foot-fall during day-time on the university

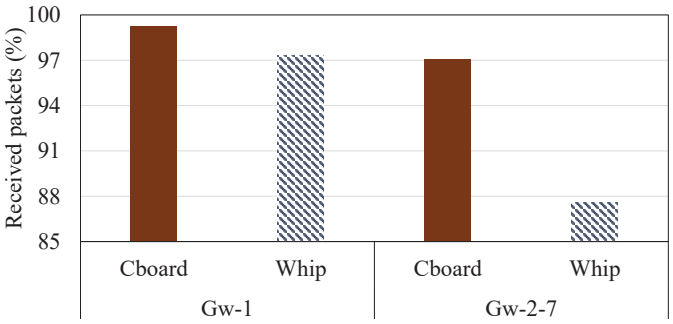

Fig. 8. Percentage of the received packets in position (a) for both the broadband cardboard (Cboard) and COTS antenna (Whip).

campus, compared to the more sub-urban position (a).

The RSS from the nodes, located in position (a), was recorded for 265 consecutive packets. The percentage of the received packets relative to those periodically transmitted every 10 s was monitored for the co-located Gw1 and the further away Gw2-6. Fig. 8 shows the percentage of received packets over the 44 minutes period. While the UWB-inspired monopole was previously found to have over 10 dB higher mean RSS for Gw1, in Fig. 6, both the whip and the UWB-inspired monopole result in under 3% missed packets. On the other hand, when observing the percentage of received packets by the further-located five gateways (Gw5-6), the node connected using a whip antenna misses over 12% of the packets. This can be attributed to the higher standard deviation in the RSS of the whip antenna, resulting in a higher CDF of the RSS under -110 dB, shown in Fig. 6.

In addition to the stationary node measurements, the path shown in Fig. 5(a) was walked at approximately 5.5 km/h from north to south. The nodes were positioned vertically, to avoid polarization misalignment, inside a user's backpack facing away from the gateways, which represents the worst-case human-shadowing scenario [7]. Observing the elevation plot in Fig. 5(b), it is expected that the shadowing introduced by the 60 m hill, approximately matching the height of Gw4-6, will have a significant influence on the RSS. The time-variant RSS between the nodes, using both antennas, and Gw4 (TTN gateway ID: b100-ttog) is shown in Fig. 9(a), with the CDF over the full journey and all gateways shown in Fig. 9(b).

From 14:22 to 14:28 in Fig. 9, the stationary nodes' RSS variations are observed which can be attributed to channel variations and the receiver's noise floor. As the nodes move higher up-hill and towards the gateway, the RSS rises by over 30 dB, peaking around -75 dB. Nevertheless, from 14:34, when walking closer to the gateways but lower in elevation, the RSS of both nodes degrades. Particularly, the moving-averaged RSS of the node connected using the COTS whip antenna drops significantly with a lower density of received packets. From the time-variant RSS, it can be seen that even though the nodes were moving closer to the gateways, the reducing elevation from 14:34 makes them more susceptible to building shadowing and subsequently the RSS drops.

The measurements performed in this study are summarized

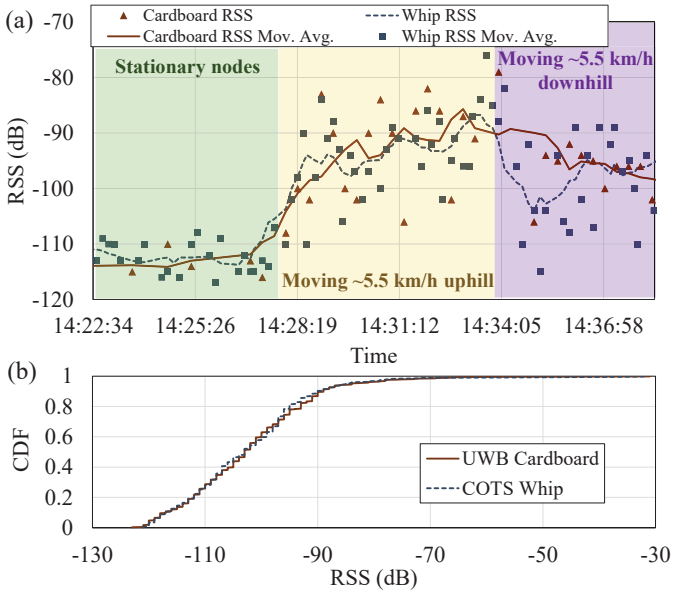

Fig. 9. The measured RSS while walking the route in Fig. 5: (a) time-varying RSS with a single gateway (Gw4); (b) CDF of the RSS across Gw1-7 over the same period.

TABLE I
PARAMETERS INVESTIGATED IN LORA PROPAGATION CAMPAIGNS

	This work	[7]	[6]	[13]	[3]
Max d	825 m	1.5 km	2.28 km	2.1 km	≈400 m
Antenna	COTS Whip; UWB	SIW	SIW	COTS, NR	COTS + dualband PCB
Elevation	✓	✗	✗	✗	✗
Time	✓	✗	✗	✓	✗
Movement	✓	✓	✓	✗	✗
Distance	✓	✓	✓	✗	✓
Multi-gateway	✓	✗	✗	✗	✗

in Table I and compared to recently reported RF propagation campaigns of LoRaWAN. As observed in the table, this work represents the only implementations where an off-the-shelf antenna design was compared through measured RSS values. Furthermore, while periodic fluctuations [13], motion-speed [7], and body-proximity effects [6], were previously studied, this work shows for the first time the effects of topological variations on the RSS, which can be more significant than distance.

IV. CONCLUSION

In this paper, LoRaWAN propagation was analyzed in an urban environment for a multitude of scenarios involving a mobile and stationary node, demonstrating that a low-cost UWB-inspired monopole antenna implemented on low-cost substrates can improve the nodes connectivity over COTS antennas. It was found that in a dense urban environment, reducing the distance between the gateway and the node does not translate to an improvement in the RSS matching theoreti-

cal LoS predictions, with over 20 dB variations. Furthermore, the effect of the node's height, e.g. due to terrain, was found to be more significant than the distance between the node and tha gateway, owing to the LoS obstructions. Finally, it was experimentally demonstrated that a reliable link can be maintained over a 1.2 km walking path with varying elevation and LoS human-shadowing.

REFERENCES

[1] H. Wang and A. O. Fapojuwo, "A survey of enabling technologies of low power and long range machine-to-machine communications," *IEEE Communications Surveys Tutorials*, vol. 19, no. 4, pp. 2621–2639, 2017.

[2] S. A. Haydhah, F. Ferrero, L. Lizzi, M. S. Sharawi, and A. Zerguine, "A multifunctional compact pattern reconfigurable antenna with four radiation patterns for sub-ghz iot applications," *IEEE Open Journal of Antennas and Propagation*, vol. 2, pp. 613–622, 2021.

[3] F. Ferrero and M. B. Toure, "Dual-band lora antenna : Design and experiments," in *2019 IEEE Conference on Antenna Measurements Applications (CAMA)*, 2019, pp. 243–246.

[4] X. Wang, L. Xing, and H. Wang, "A wearable textile antenna for lora applications," in *2021 IEEE 4th International Conference on Electronic Information and Communication Technology (ICEICT)*, 2021, pp. 613–615.

[5] P. Van Torre, T. Ameloot, and H. Rogier, "Wearable 868 mhz lora wireless sensor node on a substrate-integrated-waveguide antenna platform," in *2019 49th European Microwave Conference (EuMC)*, 2019, pp. 496–499.

[6] ——, "Long-range body-to-body lora link at 868 mhz," in *2019 13th European Conference on Antennas and Propagation (EuCAP)*, 2019, pp. 1–5.

[7] T. Ameloot, P. Van Torre, and H. Rogier, "Lora base-station-to-body communication with simo front-to-back diversity," *IEEE Transactions on Antennas and Propagation*, vol. 69, no. 1, pp. 397–405, 2021.

[8] J. Liang, C. Chiau, X. Chen, and C. Parini, "Study of a printed circular disc monopole antenna for uwb systems," *IEEE Trans. Antennas Propag.*, vol. 53, no. 11, pp. 3500 – 3504, 2005.

[9] M. Wagih, A. S. Weddell, and S. Beeby, "Omnidirectional Dual-Polarized Low-Profile Textile Rectenna with over 50% Efficiency for Sub-μW/cm^2 Wearable Power Harvesting," *IEEE Transactions on Antennas and Propagation*, vol. 69, no. 5, pp. 2522–2536, 2021.

[10] M. Wagih and T. Moody, "Open-Source Low-Cost Antenna Measurement Setup for Rapid Echoic Measurements," *IEEE International Conference on Antenna Measurements and Applications (CAM)*, 2021.

[11] C. A. Balanis, "Antenna Theory: Analysis and Design. Third Edition," *Wiley Interscience*, pp. 84 – 85, 2005.

[12] N. R. Harris and J. Curry, "Development and Range Testing of a LoRaWAN System in an Urban Environment," *International Journal of Electrical, Electronic and Communication Sciences*, vol. 11.0, no. 1, Jan. 2018. [Online]. Available: https://doi.org/10.5281/zenodo.1315517

[13] T. Ameloot, P. Van Torre, and H. Rogier, "Periodic lora signal fluctuations in urban and suburban environments," in *2019 13th European Conference on Antennas and Propagation (EuCAP)*, 2019, pp. 1–5.